Available online at www.sciencedirect.com
ScienceDirect
Trans. Nonferrous Met. Soc. China 25(2015) 2490−2498
Transactions of Nonferrous Metals Society of China
www.tnmsc.cn

Comparison of microstructure and wear resistance of A356−SiC_p composites processed via compocasting and vibrating cooling slope

H. KHOSRAVI, F. AKHLAGHI

School of Metallurgy and Materials Engineering, College of Engineering,
University of Tehran, P. O. Box 11155-4563, Tehran, Iran

Received 9 October 2014; accepted 2 February 2015

Abstract: The influences of SiC content on the microstructure, porosity, hardness and wear resistance of A356−SiC_p composites processed via two different methods of compocasting and vibrating cooling slope (VCS) were compared with each other. In the as-cast condition, the matrix of VCS and compocast processed composites exhibited globular and dendritic structures, respectively. While a more uniform distribution of SiC particulates in the matrix alloy as well as higher hardness values were obtained for the VCS processed samples, the composites produced via compocasting exhibited less porosity. The increased SiC content (up to 20% in volume fraction) resulted in a more uniform distribution of SiC particles within the matrix alloy and improved wear resistance for both the composite series. However, for the VCS processed composites, the increased SiC content, resulted in the decreased size and shape factor of globules as well as better tribological properties when compared with compocast composites. It was concluded that the improved properties of the VCS processed composites when compared with their compocast counterparts was a consequence of a more uniform distribution of SiC particulates in the matrix alloy as well as the globular microstructure generated during the VCS process.

Key words: Al−A356/SiC_p composite; compocasting; vibrating cooling slope; microstructure; particle distribution; porosity; hardness; wear resistance

1 Introduction

Al/SiC_p composites, due to their low density, low coefficient of thermal expansion, high specific strength and stiffness and good wear resistance, have recently gained applications in automotive and aerospace industries [1−4]. These composites can be fabricated via numerous processes such as powder metallurgy [5,6], infiltration [7], spray deposition [8], and compocasting [9−11]. Compocasting is a semi-solid processing route in which the ceramic reinforcing particulates are incorporated to the semi-solid matrix alloy via mechanical stirring, resulting in a globular structure [10,11]. Some other semi-solid processes for obtaining globular structures in aluminum alloys include mechanical vibration [12,13], mechanical stirring [14], twin screw reheomolding [15], new reheocasting [16] and cooling slope techniques [17−20]. Recently, an innovative process termed as vibrating cooling slope (VCS) method was developed to create globular structures in Al alloys. This technique is a combination of two semi-solid processes, namely cooling slope and mechanical vibration. In this method, molten metal is poured on an inclined plate and mechanical vibration is applied to it simultaneously. The VCS technique has a number of advantages over conventional semi-solid casting processes, such as simplicity, lower cost, refined microstructure and improved mechanical properties. Also, in contrast to the stationary cooling slope method in which the globular structure can only be achieved after re-heating the samples, the VCS is a single-step process that generates a globular structure in the as-cast condition [21−24].

There exist some conflicting reports in the literature about the effect of SiC particles on the microstructure of the matrix alloy in the cast Al−SiC composites. Our previous studies revealed the refinement of grain size in the A356−SiC_p composites as compared with the matrix alloy [11]. This effect was intensified for increased SiC content. However, ROHATGI et al [25] reported an increase in the dendrite arm spacing (DAS) in A356

Corresponding author: F. AKHLAGHI; E-mail: fakhlagh@ut.ac.ir
DOI: 10.1016/S1003-6326(15)63867-5

aluminum alloys as a result of SiC addition. On the other hand, the results of some studies indicate the negligible effect of SiC particles on the microstructure of cast A356−SiC_p composites [26,27].

The optimum properties in the metal matrix composites (MMCs) can be achieved when the reinforcing particles are distributed uniformly within the matrix alloy. A non-homogeneous particle distribution in the cast MMCs often arises as a result of agglomeration, settling and segregation of ceramic particles during casting [28−30] that are influenced by several factors such as the wettability of the particles with the molten alloy, proper mixing, reinforcement size and content, mold temperature and solidification rate [10,31]. It has been reported that particle clustering can be minimized by increasing the solidification rate [32,33]. Particle clusters act as crack nucleation sites at stresses lower than the matrix yield strength, causing the material to fail at unpredictable low stress levels [34].

The porosity in the cast particulate MMCs is another problem and has been related to the particle size and content, mold temperature, and processing route [10,35,36].

Al/SiC_p composites have generally exhibited improved wear resistance over the base alloy. The wear behavior of MMCs has been found to be a function of different factors such as reinforcement volume fraction, particle size, and applied load [10,11,31,37,38]. The nature and properties of the interface between the reinforcing phase and the matrix are affected by composite fabrication method and can influence the wear properties of the material. For example, our previous study on the wear behavior of A356−SiC_p composites produced via two different versions of compocasting processes revealed that the composites with a globular structure exhibited the improved wear properties [10].

The aim of the present study is to compare the microstructural characteristics, porosity, hardness and wear resistance of A356−SiC_p composites processed via compocasting and VCS routes.

2 Experimental

Al−Si casting alloy (A356) with nominal compositions (mass fraction, %) of balance Al, 6.93 Si, 0.23 Mn, 0.26 Zn, 0.38 Mg, 0.25 Cu and 0.11 Fe was used as the matrix material. The relatively large freezing range of this alloy (32 °C) makes it suitable for semi-solid processing. Silicon carbide (SiC) particles in the size range of 63−90 μm (average size 76 μm) were used as the reinforcing material.

The VCS apparatus, as shown schematically in Fig. 1, consists of a cooling slope made of copper plate (1000 mm × 120 mm × 10 mm) mounted on a steel frame. This assembly was fixed on a steel plate and could vibrate at different frequencies by means of a 3HP, 2840 r/min electrical motor. More details about this apparatus can be found in Ref. [21].

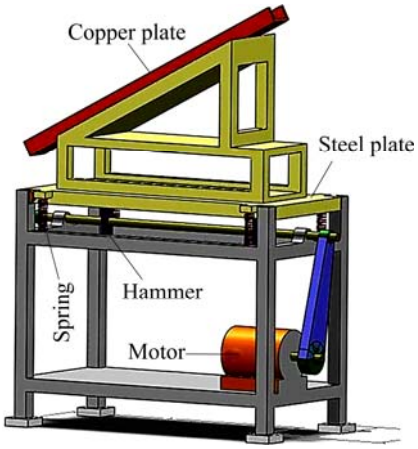

Fig. 1 Schematic representation of VCS apparatus used in this study

Al−SiC_p composites with various contents of SiC particles (5%, 10%, 15% and 20%, volume fraction) were fabricated by both the compocasting and VCS methods. The SiC particles were initially oxidized in air at 1000 °C for a period of 120 min. This process resulted in formation of a layer of SiO_2 on the surface of particles and improved their wettability with molten aluminum.

The matrix alloy was melted and then its temperature was decreased to about 590 °C while stirred at 800 r/min using a graphite impeller attached to a motor. At this stage, specific amounts of oxidized SiC particles were added to the alloy at a rate of 50 g/min and the semi-solid slurry was stirred for 20 min to obtain a uniform distribution of the SiC particles in the matrix. In order to facilitate the casting of slurry, it was heated to 670 °C and stirred at this temperature for another 5 min. For producing the compocasting samples, the resultant slurry was poured into a cast-iron die with the internal diameter of 80 mm and a height of 60 mm. The VCS samples were made by pouring the Al/SiC slurry onto the surface of the cooling slope set at 45° inclined angle while it was vibrated at 65 Hz of frequency and 680 μm of amplitude. After travelling the distance of 400 mm on the cooling slope, the melt was poured into the same cast-iron die as mentioned before. Our previous investigations revealed that this set of processing condition for A356 aluminum alloy resulted in formation of the most spherically shaped α-Al globules [21].

The samples for metallographic investigations were cut from the geometrical center of the produced composite ingots, as shown in Fig. 2. These samples were subjected to standard metallographic procedures, etched in 0.5% HF acid solution for 13 s and examined

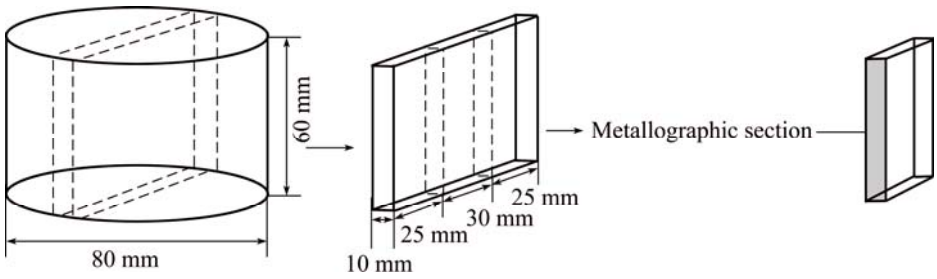

Fig. 2 Position of metallographic samples in cast ingot

via an Olympus-BX60M light microscope.

The equivalent diameter (D_e) and shape factor (F_S) of the globules were calculated using Eqs. (1) and (2), respectively [39].

$$D_e = \frac{\sum_1^N \sqrt{\frac{4A}{\pi}}}{N} \quad (1)$$

$$F_S = \frac{\sum_1^N \frac{4\pi A}{P}}{N} \quad (2)$$

where A and P are the area and perimeter of globules, respectively and N is the total number of randomly selected globules for each sample. A and P for 100 globules (N=100) were calculated using microstructural image processing (MIP) software. F_S is a number indicating the degree of sphericity of globules and varies in the range of 0−1.

The distribution of the SiC particles within the matrix alloy was quantified by considering a factor termed as distribution factor (F_D) calculated using the following equation [40]:

$$F_D = \frac{\sigma}{A_f} \quad (3)$$

where A_f is the mean value of the area fraction of the SiC particles measured on 100 fields of a sample and σ is its standard deviation. The smaller F_D indicates the more uniform distribution of SiC particles in the matrix alloy.

The density of the samples was measured using the Archimedes' principle. The measured density was compared with that obtained using rule-of-mixtures so as to determine the volume fraction of porosity. The samples were precisely weighed in an electronic balance to an accuracy of 0.1 mg. Hardness measurements were carried out on a Brinell hardness testing machine using a load of 300 N. The mean values of at least five measurements conducted on different areas of each sample were considered.

Pin-on-disk dry sliding wear tests were carried out at ambient laboratory conditions using a steel pin (1.5Cr, 1C, 0.35Mn, 0.25Si) with the hardness of HRC 64, diameter of 5 mm and height of 20 mm. The applied load on the pin was 20 N resulting in 1 MPa pressure and the sliding velocity was 0.5 m/s. The tests were interrupted at sliding distance of 1000 m and the incremental mass loss of the sample was recorded. After each increment (and before weighing), the pin and disk were cleaned in an ultrasonic bath with acetone and hot-wind dried below 100 °C. The worn surfaces were examined using a Camscan MV2300 scanning electron microscope (SEM).

3 Results and discussion

Figure 3 shows typical optical micrographs of the base alloy and the A356−20%SiC_p (volume fraction) composite prepared via the compocasting process. The dendritic structure of the base alloy is preserved in the matrix of the composite and the SiC particles are pushed to the interdendritic regions.

The optical micrographs of the base alloy and the A356−20%SiC_p composite both processed via the VCS process are compared with each other in Fig. 4. In agreement with our previous studies for monolithic aluminum alloy [21], the well defined α-Al globules are dispersed in the eutectic phase as shown in Fig. 4(a). According to Fig. 4(b) at the presence of 20% SiC particles, the globular structure has been preserved. However, less spherical shaped globules are generated in the composite sample. The formation of the globular structure in the VCS-processed samples is attributed to the generation of numerous nuclei during flow of the slurry over the vibrating cooling plate. These nuclei are detached from the surface of the cooling slope as a result of simultaneous applying mechanical vibration and melt flow. The presence of these nucleation sites in the solidifying melt results in generation of a globular microstructure in the as-cast ingot.

Figure 5(a) shows the decreased average sizes (D_e) of the globules with increased SiC content. These results are in agreement with other reports [11,41] and can be explained as follows: The increased content of SiC particles in the solidifying slurry can alter the matrix microstructure due to the decreased latent heat released during solidification resulting in decreased solidification

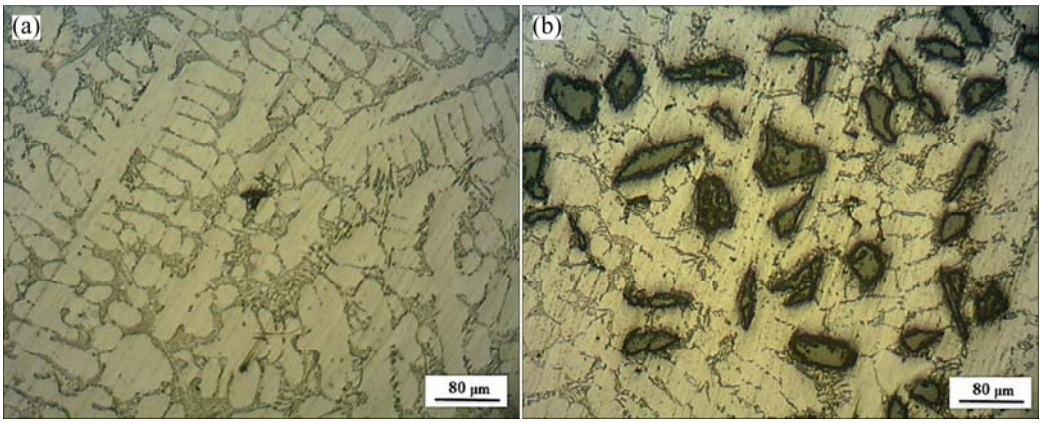

Fig. 3 Typical optical micrographs of base alloy (a) and A356−20%SiC_p composite (b) prepared via compocasting process

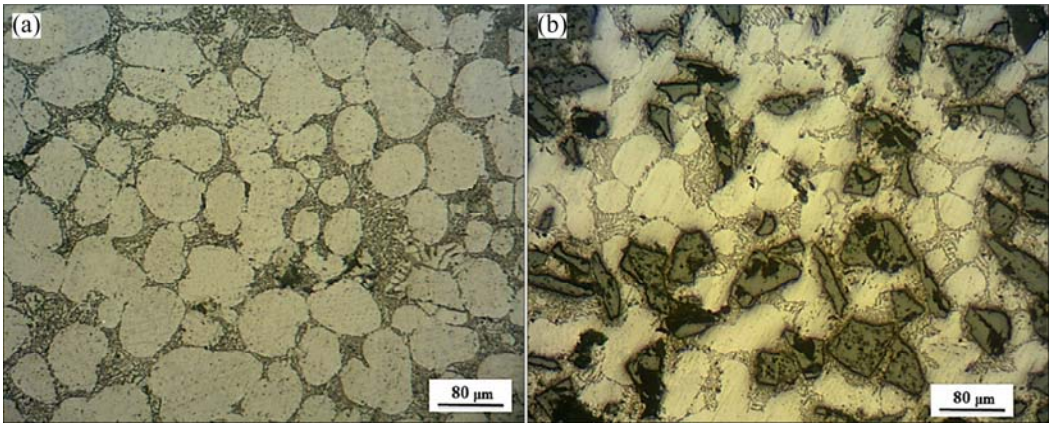

Fig. 4 Typical optical micrographs of base alloy (a) and A356−20%SiC_p composite (b) via VCS process

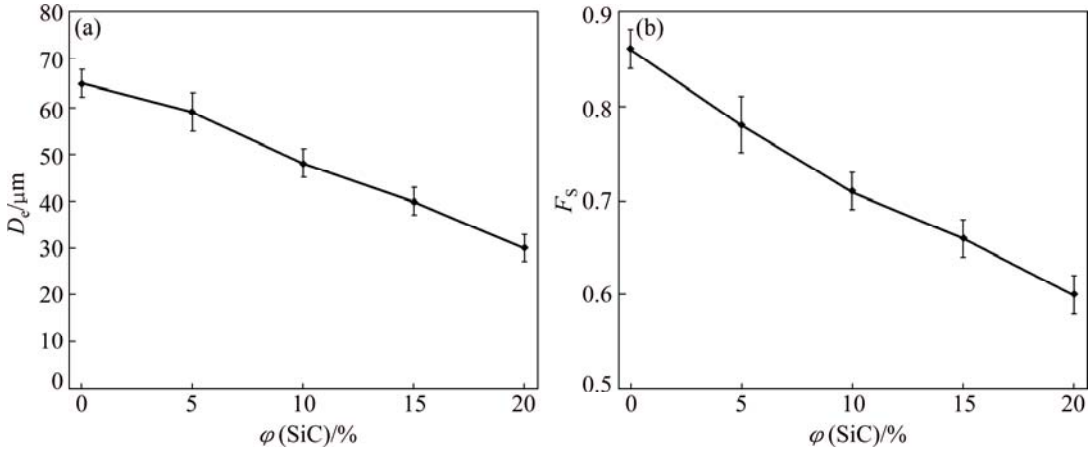

Fig. 5 Variation of average size (D_e) (a) and shape factor (F_S) (b) of globules with SiC content for samples processed via VCS method

time and increased solidification rate, the increased surface area of SiC particles resulting in increased barriers for the growth of α-Al phase, and the increased shear forces applied to the semi-solid alloy intensifying fragmentation of dendrites resulting in generation of more nucleation sites. Figure 5(b) shows the decreased shape factor, indicating the formation of less spherically shaped globules, with increased SiC content. These results are in agreement with Fig. 4(b) and can be partially attributed to the increased solidification rate for the increased SiC content. This in turn shortens the available time for the α-Al phase to gain a spherical shape before the end of solidification. In addition, sticking of SiC particles to the solidifying α-Al globules restricts their free spherodization under the surface tension forces.

Figure 6 reveals the effect of SiC content on the distribution of particles within the matrix alloy for both the compocast and VCS-processed composite series. It can be seen that the increased SiC content resulted in a more homogeneous distribution of these particles within the matrix alloy for both the sample series as indicated by smaller F_S values. These results can be attributed to the increased solidification rate and refined microstructure with increased SiC content.

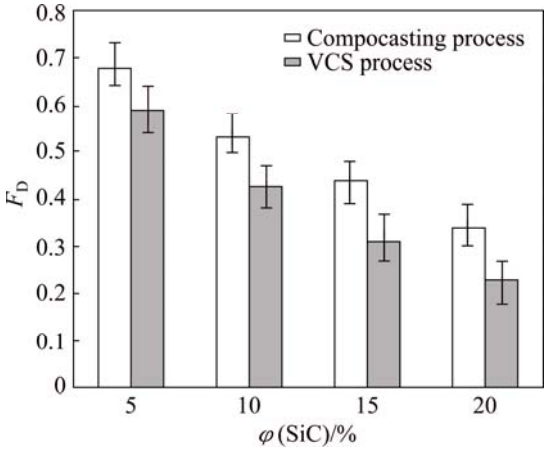

Fig. 6 Effect of SiC content on distribution factor in compocasting and VCS-processed samples

According to Fig. 6, in the VCS-processed samples, the SiC particles were more uniformly distributed as compared with their compocast counterparts at any SiC particle content. These results are confirmed by comparing the optical micrographs of A356−10% SiC composites in Fig. 7 and can be attributed to the decreased solidification time and retarded segregation of the SiC particles in the VCS-processed samples.

The increased porosity with the increase of SiC content in compocasting and VCS-processed samples is shown in Fig. 8. These results are in agreement with other reports [10,31,35,36] and can be attributed to a number of reasons as follows: 1) the increased amount of gas entering the melt via gas layers on the surface of SiC particles; 2) the increased effective viscosity of the slurry resulting in a higher gas entrapment; 3) the increased SiC particle clustering and air trapping in the cluster of particles as well as the hindered liquid metal flow inside them; and 4) the increased sites for heterogeneous pore nucleation. Figure 8 also reveals that at any SiC particle content, the VCS-processed samples are always more porous than their compocast counterparts. Again, the shorter solidification time in the VCS process reduced the available time for gas escape and resulted in increased porosity level. In addition, the turbulent flow of slurry on the cooling slope intensified the entrance of air in the melt and part of this air bubbles remained in the composite as porosity.

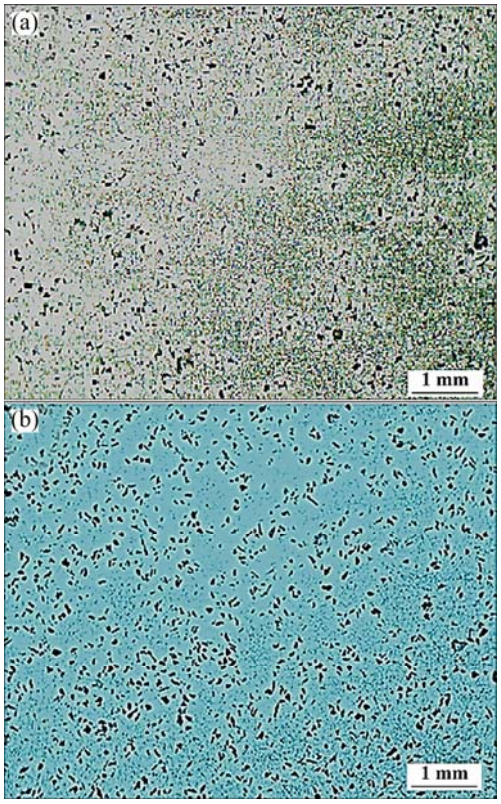

Fig. 7 Optical micrographs of A356−10% SiC composites processed via compocasting (a) and VCS (b) methods

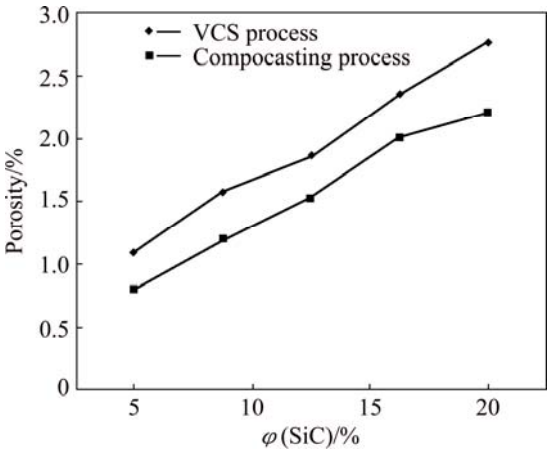

Fig. 8 Variation of porosity level with SiC content in compocasting and VCS-processed samples

The increased hardness with SiC content in both composite series is shown in Fig. 9 (a). These results are in agreement with other studies [31,42,43] and can be attributed to the increased content of a hard phase (SiC) in the composites. In addition, the presence of SiC particles alters the matrix microstructure via several mechanisms. As shown in Fig. 9(b), the increased SiC content resulted in decreased aspect ratio of eutectic Si phase for both composite series. This effect can be explained by the increased shear forces applied to the

semi-solid alloy resulting in generation of more nucleation sites as well as the increased solidification rate. Also, the increased SiC content results in increased dislocation density within the matrix alloy due to the mismatch in the coefficients of thermal expansion of SiC and aluminum alloy. The combination of these effects improves the yield strength and hardness of composites. These results are consistent with some related studies [11,38].

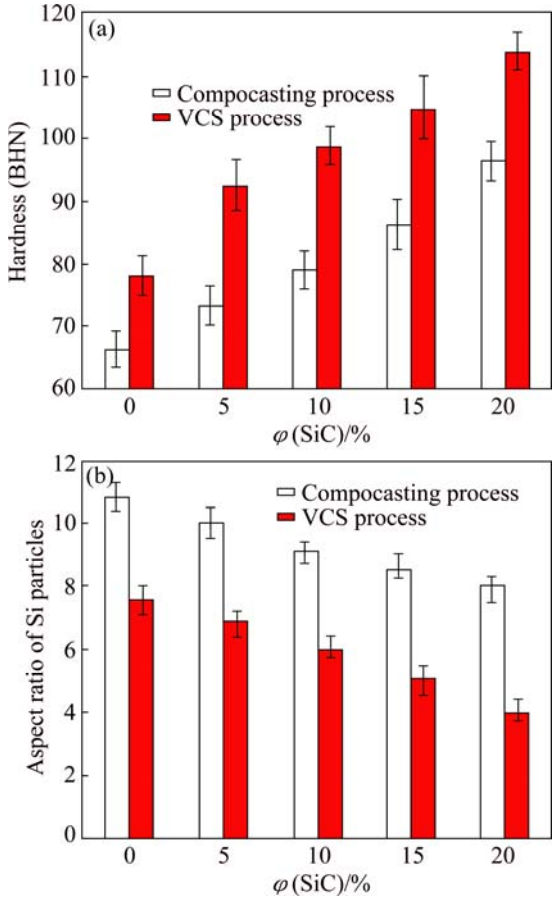

Fig. 9 Variation of hardness (a) and aspect ratio of eutectic Si particles (b) with SiC content for compocasting and VCS-processed samples

Figure 9(a) reveals higher hardness values of the VCS-processed samples as compared with their compocast counterparts at any SiC particle content. These results can be attributed to the different microstructures of these two composite series as explained before and smaller aspect ratio of eutectic Si particles in VCS-processed samples (Fig. 9(b)).

The decreased wear rate with increased SiC content for both composite series is presented in Fig. 10. These results are consistent with the trends reported by other authors [10,11,31,37,38] and can be partially attributed to the increased hardness of the composites. According to the Archard theory [44], wear resistance is proportional to the hardness of material. It can be seen that despite the higher porosity of VCS-processed samples (Fig. 8), they exhibit higher hardness (Fig. 9(a)) and lower wear rate (Fig. 10) as compared with their compocast counterparts, at any SiC particle content. These results are in agreement with our previous study [10] and can be attributed to the different microstructures of these two differently processed composite series, as mentioned before, as well as a more uniform distribution of SiC particles in the matrix of the VCS processed composites.

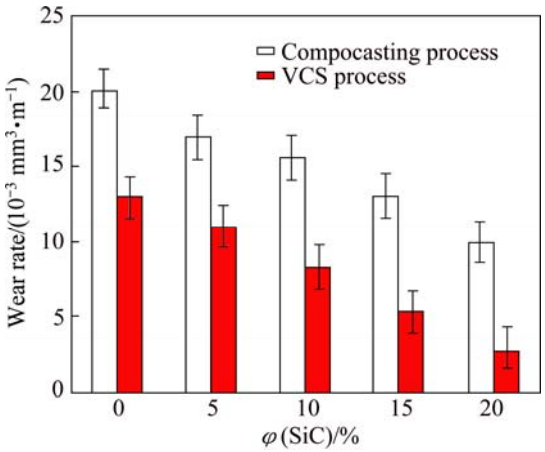

Fig. 10 Variation of wear rate with SiC content for compocasting and VCS-processed samples

The SEM micrographs of the worn surfaces of the A356−10% SiC composite processed via compocasting and VCS methods are shown in Fig. 11. According to Fig. 11(a), plastic deformation occurred during wear test of compocast-processed sample, indicating the adhesive wear mechanism. This was accompanied with deep groves observed on the worn surface of this sample (Fig. 11(b)) interspersed by craters (Fig. 11(a)). However, for the VCS-processed sample, abrasive wear was the predominant wear mechanism (Fig. 11(c)) and the worn surface of the composite was relatively smooth, exhibiting some shallow grooves (Fig. 11(d)). This behavior can be explained by the higher hardness of the VCS-processed composite (Fig. 9) and its increased yield strength that prevented plastic deformation during wear test.

The decreased coefficients of friction with increased SiC content for both composite series are shown in Fig. 12. These results though consistent with the trend reported in Refs. [45,46] are opposite to those observed by SINGLA et al [47] and can be attributed to the variations in the microstructure (Figs. 5, 6, 8 and 9(b)), hardness (Fig. 9(a)), porosity (Fig. 8) and mechanical properties of the composites with the SiC content. For example, the increased hardness of composites with increased SiC content can be partially responsible for the observed decreased friction coefficient. Also, it has been reported that the porosity content can be regarded as

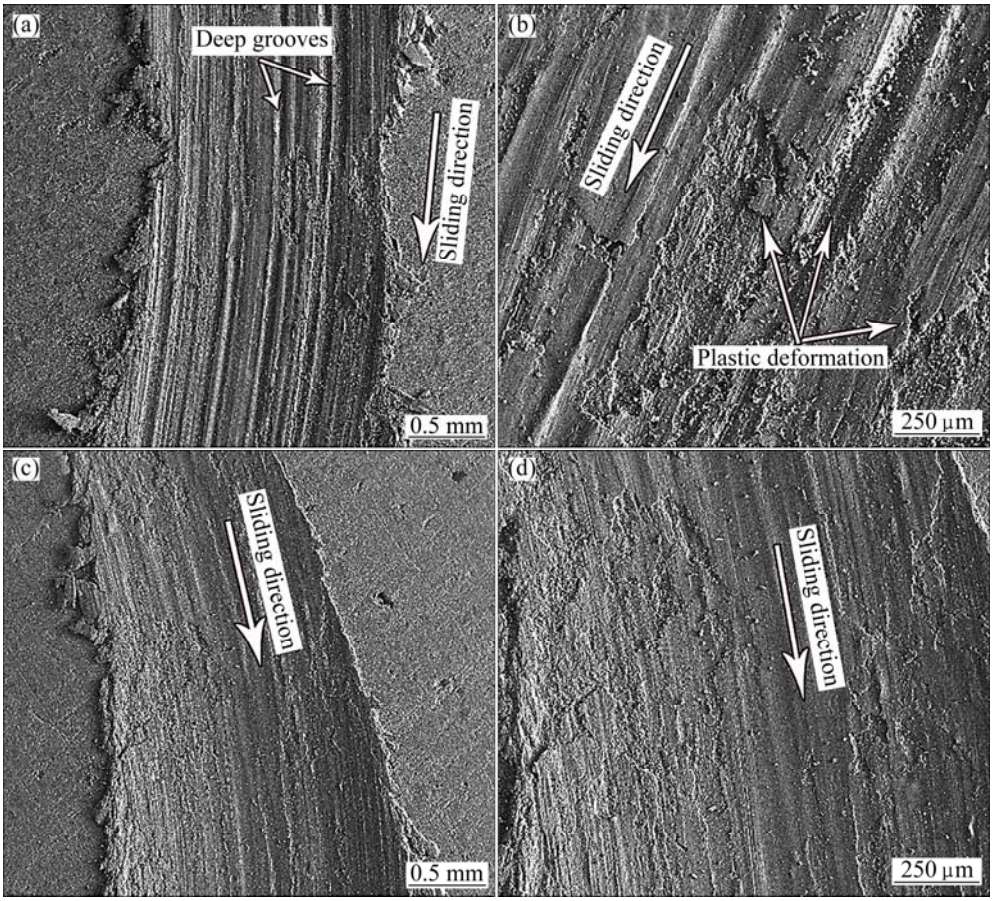

Fig. 11 Worn surfaces of A356−10%SiC_p composites prepared by different methods: (a, b) Compocasting; (c, d) VCS

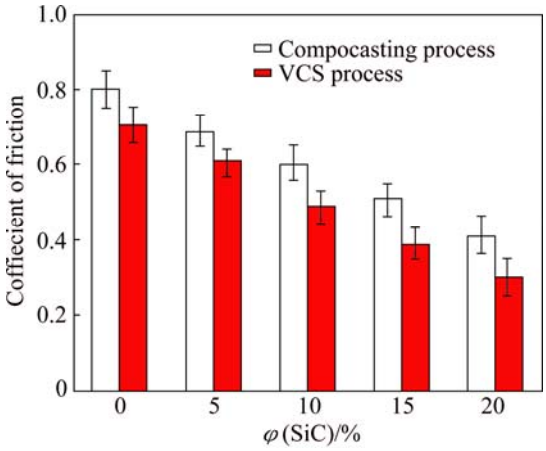

Fig. 12 Variation in coefficient of friction with SiC content for compocast and VCS processed samples

an important factor in decreasing the friction coefficient [48]. Figure 12 also reveals a lower coefficient of friction for VCS-processed samples at any SiC particle content as compared with the compocast-processed samples. Again, these results are consequences of different microstructures and mechanical properties of these two composite series that result in different wear mechanisms and friction coefficient values. Particularly, the tendency of compocast-processed samples for plastic deformation during wear test as well as their lower hardness values and lower porosity are responsible for their higher friction coefficients.

4 Conclusions

1) The matrix of compocast-processed composites exhibited a dendritic structure while the SiC particles were pushed to the interdendritic regions. In the as-cast VCS composites, the SiC particles were dispersed uniformly between the globules of α-Al phase. The increased SiC content resulted in decreased size at the expense of decreased sphericity of globules. For both the compocasting and VCS samples, the uniformity in the SiC distribution improved with increasing the SiC content. However, the SiC particles in the VCS samples were more uniformly distributed as compared with their compocast counterparts at any SiC particle loading.

2) The increased SiC content resulted in decreased aspect ratio of eutectic silicon particles, increased porosity level and increased hardness of both the compocast and VCS samples. However, despite of the higher porosity content of the VCS samples, they exhibited higher hardness values at any SiC particle content when compared with their compocast

counterparts.

3) The increased SiC content resulted in decreased wear rate and friction coefficient of both the compocast and VCS samples. However, at any SiC particle loading, the VCS-processed samples exhibited lower wear rates and smaller friction coefficients as compared with their compocast counterparts. These observations were attributed to the different microstructures of these two differently processed composite series (i.e., smaller aspect ratio of eutectic Si particles, higher porosity as well as a more uniform distribution of SiC particles in the matrix alloy in the VCS-processed samples) together with a higher hardness that resulted in improved tribological properties.

References

[1] LLOYD D J. Particle reinforced aluminum and magnesium matrix composites [J]. International Materials Review, 1994, 39(1): 1−21.

[2] CHAWLA N, CHAWLA K K. Metal matrix composites [M]. New York: Springer, 2006.

[3] SONG Min. Effects of volume fraction of SiC particles on mechanical properties of SiC/Al composites [J]. Transactions of Nonferrous Metals Society of China, 2009, 19(6): 1400−1404.

[4] MAZAHERY A, OSTAD SHABANI M. Microstructural and abrasive wear properties of SiC reinforced aluminum-based composite produced by compocasting [J]. Transactions of Nonferrous Metals Society of China, 2013, 23(7): 1905−1914.

[5] MAHDAVI S, AKHLAGHI F. Fabrication and characteristics of Al6061/SiC/Gr hybrid composites processed by in situ powder metallurgy method [J]. Journal of Composite Materials, 2013, 47: 437−447.

[6] LIU Z Y, WANG Q Z, XIAO B L, MA Z Y, LIU Y. Experimental and modeling investigation on SiC_p distribution in powder metallurgy processed SiC_p/2024 Al composites [J]. Materials Science and Engineering A, 2010, 527: 5582−5591.

[7] ALTINKOK N. Microstructure and tensile strength properties of aluminum alloys composites produced by pressure-assisted aluminum infiltration of Al_2O_3/SiC preforms [J]. Journal of Composite Materials, 2004, 38: 1533−1543.

[8] CHEN Zhi-gang, CHEN Zhen-hua, CHEN Ding, HE Yi-qiang, CHEN Gang. Microstructural evolution and its effects on mechanical properties of spray deposited SiC_p/8009Al composites during secondary processing [J]. Transactions of Nonferrous Metals Society of China, 2009, 19(5): 1116−1120.

[9] ABBASIPOUR B, NIROUMAND B, MONIR VAGHEFI S M. Compocasting of A356-CNT composite [J]. Transactions of Nonferrous Metals Society of China, 2010, 20(9): 1561−1566.

[10] AKHLAGHI F, LAJEVARDI A, MAGHANAKI H M. Effects of casting temperature on the microstructure and wear resistance of compocast A356/SiC_p composites: A comparison between SS and SL routes [J]. Journal of Materials Processing and Technology, 2004, 155−156: 1874−1880.

[11] AKHLAGHI F, ZAHEDI H, SHARIFI M. Effect of reinforcement volume fraction, reinforcement size and solution heat treatment on the microstructure of the two differently processed A356/SiC_p composites [J]. Iranian Journal of Materials Science and Engineering, 2004, 1: 13−22.

[12] TAGHAVI F, SAGHAFIAN H, KHARRAZI Y H. Study on the effect of prolonged mechanical vibration on the grain refinement and density of A356 aluminum alloy [J]. Materials and Design, 2009, 30: 1604−1611.

[13] WU Shu-sen, XIE Li-zhi, ZHAO Jun-wen, NAKAE H. Formation of non-dendritic microstructure of semi-solid aluminum alloy under vibration [J]. Scripta Materialia, 2008, 58(7): 556−559.

[14] RAHIMI B, KHOSRAVI H, HADDAD-SABZEVAR M. Microstructural characteristics and mechanical properties of Al-2024 alloy processed via a rheocasting route [J]. International Journal of Minerals, Metallurgy and Materials, 2015, 22: 59−67.

[15] JI S, FAN Z, BEVIS M J. Semi-solid processing of engineering alloys by a twin screw rheomolding process [J]. Materials Science and Engineering A, 2001, 299: 210−217.

[16] CARDOSO E, ATKINSON H V, JONES H. Microstructural evolution of A356 during NRC processing [C]//Proceedings of the 8th International Conference on Semi-Solid Processing of Alloys and Composites. Limassol: University of Cyprus, 2004.

[17] SAKLAKOGLU N, GENCALP S, KASMAN S. The effects of cooling slope casting and isothermal treatment on wear behavior of A380 alloy [J]. Advanced Materials Research, 2011, 264−265: 42−47.

[18] KUND N K, DUTTA P. Numerical simulation of solidification of liquid aluminum alloy flowing on cooling slope [J]. Transactions of Nonferrous Metals Society of China, 2010, 20(S): s898−s905.

[19] KHOSRAVI H, ESLAMI-FARSANI R, ASKARI-PAYKANI M. Modeling and optimization of cooling slope process parameters for semi-solid casting of A356 Al alloy [J]. Transactions of Nonferrous Metals Society of China, 2014, 24(4): 961−968.

[20] HAGA T, NAKAMURA R, TAGO R, WATARI H. Effects of casting factors of cooling slope on semisolid condition [J]. Transactions of Nonferrous Metals Society of China, 2010, 20(S): s968−s972.

[21] AKHLAGHI F, TAGHANI A. Development of vibrating cooling slope (VCS) method for enhancing a globular structure in aluminum A356 alloy [C]//Proceedings of the 12th International Conference on Aluminum Alloys. Yokohama, Japan: The Japan Institute of Light Metals, 2010: 1839−1844.

[22] GUAN R G, CAO F R, CHEN L Q, LI J P, WANG C. Dynamical solidification behaviors and microstructural evolution during vibrating wavelike sloping plate process [J]. Journal of Materials Processing and Technology, 2009, 209: 2592−2601.

[23] LIU W, TAN J, LI J, DING X. Influence of process parameters by vibrational cooling-shearing slope on microstructures of semi-solid ZAlSi9Mg alloy [J]. Advanced Materials Research, 2011, 211−212: 142−146.

[24] GENCALP S, SAKLAKOGLU N. Semisolid microstructure evolution during cooling slope casting under vibration of A380 aluminum alloy [J]. Materials and Manufacturing Processing, 2010, 25: 943−947.

[25] ROHATGI P K, PASCIAK K, NARENDRANATH C S, RAY S. Evolution of microstructure and local thermal conditions during directional solidification of A356−SiC particle composites [J]. Mater Sci, 1994, 29: 5357−5366.

[26] LLOYD D J. Solidification behavior of particulate reinforced aluminum/SiC composites [J]. Composite Science and Technology, 1989, 35: 159−579.

[27] NAGARAJAN S, DUTTA B, SURAPPA M K. The effect of SiC particles on the size and morphology of eutectic silicon in cast A356/SiC_p composites [J]. Composite Science and Technology, 1999, 59: 897−902.

[28] OURDJINI A, CHEW K, KHOO C. Settling of silicon carbide particles in cast metal matrix composites [J]. Journal of Materials Processing and Technology, 2001, 116: 72−76.

[29] SOHRABI BABA HEIDARI D, AKHLAGHI F. Theoretical and Experimental study on settling of SiC particles in composite slurries of aluminum A356/SiC [J]. Acta Materialia, 2011, 59: 4556−4568.

[30] MAHENDRA K V, RADHAKRISHNA K. Characterization of stir cast Al−Cu−(fly ash + SiC) hybrid metal matrix composites [J]. Journal of Composite Materials, 2010, 44: 989−1005.
[31] VUGT L V, FROYEN L. Gravity and temperature effects on particle distribution in Al−Si/SiC_p composites [J]. Journal of Materials Processing and Technology, 2000, 104: 133−144.
[32] CETIN A, KALKANLI A. Numerical simulation of solidification kinetics in A356/SiC_p composites for assessment of as-cast particle distribution [J]. Journal of Materials Processing and Technology, 2009, 209: 4795−4801.
[33] CETIN A, KALKANLI A. Effect of solidification rate on spatial distribution of SiC particles in A356 alloy composites [J]. Journal of Materials Processing and Technology, 2008, 205: 1−8.
[34] HONG S J, KIM H M, HUH D, SURYANARAYANA C, CHUN B S. Effect of clustering on the mechanical properties of SiC particulate-reinforced aluminum alloy 2024 metal matrix composites [J]. Materials Science and Engineering A, 2003, 347: 198−204.
[35] AHMAD S N, HASHIM J, GHAZALI M I. Effect of porosity on tensile properties of cast particle reinforced MMC [J]. Journal of Composite Materials, 2007, 41: 575−589.
[36] AHMAD S N, HASHIM J, GHAZALI M I. The effects of porosity on mechanical properties of cast discontinuous reinforced metal-matrix composite [J]. Journal of Composite Materials, 2005, 39: 451−466.
[37] MAHDAVI S, AKHLAGHI F. Effect of the SiC particle size on the dry sliding wear behavior of SiC and SiC−Gr reinforced Al6061 composites [J]. Mater Sci, 2011, 46: 7883−7894.
[38] AKHLAGHI F, MAHDAVI S. Effect of the SiC content on the tribological properties of hybrid Al/Gr/SiC composites processed by in situ powder metallurgy (IPM) method [J]. Advanced Materials Research, 2011, 264−265: 1878−1886.
[39] SEO P K, KANG C G. The effect of raw material fabrication process on microstructural characteristics in reheating process for semi-solid forming [J]. Journal of Materials Processing and Technology 2005, 162−163: 402−409.
[40] RAHMANI R, AKHLAGHI F. Effect of extrusion temperature on the microstructure and porosity of A356−SiC_p composites [J]. Journal of Materials Processing and Technology, 2007, 187−188: 433−436.
[41] MUSTAFA S F. Casting of graphitic Al−Si base composites [J]. Canadian Metallurgical Quarterly, 1994, 33: 259−264.
[42] SINGLA M, DWIVWDI D D, SINGH L, CHAWLA V. Development of aluminum based silicon carbide particulate metal matrix composite [J]. Journal of Minerals and Materials Characterization, 2009, 8: 455−467.
[43] BEDIR F. Characteristic properties of Al−Cu−SiC_p and Al−Cu−B_4C_p composites produced by hot pressing method under nitrogen atmosphere [J]. Materials and Design, 2007, 28: 1238−1244.
[44] HUTCHINGS I M. Tribology: Friction and wear of materials [M]. London: Edward Arnold, 1992.
[45] MAHDAVI S, AKHLAGHI F. Effect of SiC content on the processing, compaction behavior, and properties of Al6061/SiC/Gr hybrid composites [J]. Mater Sci, 2011, 46: 1502−1511.
[46] HASSAN A M, ALRASHDAN A, HAYAJNEH M T, MAYYAS A T. Wear behavior of Al−Mg−Cu-based composites containing SiC particles [J]. Tribol Int, 2009, 42: 1230−1238.
[47] SINGLA M, SINGH L, CHAWLA V. Study of wear properties of Al−SiC composites [J]. Journal of Minerals and Materials Characterization, 2009, 8: 813−819.
[48] TEOH S H, THAMPURAN R, SEAH W. Coefficient of friction under dry and lubricated conditions of a fracture and wear resistant P/M titanium−graphite composite for biomedical applications [J]. Wear, 1998, 214: 237−244.

复合铸造与振动斜板冷却铸造 SiC_p 增强 A356 复合材料显微组织与耐磨性的比较

H. KHOSRAVI, F. AKHLAGHI

School of Metallurgy and Materials Engineering, College of Engineering,
University of Tehran, P. O. Box 11155-4563, Tehran, Iran

摘　要：利用复合铸造和振动斜板铸造 2 种方法铸造 SiC_p 增强 A356 复合材料，比较 2 种复合材料中碳化硅含量对材料显微组织、孔隙、硬度和耐磨性的影响。在铸态条件下，振动斜板铸造和复合铸造的 2 种复合材料的基体分别为球形和枝晶结构。 振动斜板铸造的复合材料其碳化硅颗粒分布更加均匀，并且具有更高的硬度，复合铸造的材料则具有更少的孔隙。对于这 2 种复合材料，碳化硅颗粒的增加(体积分数最大为 20%)导致碳化硅颗粒在基体合金内更加均匀分布并且提高了其耐磨性。与复合铸造材料相比，对于振动斜板铸造的复合材料，碳化硅含量的增加，将降低球形颗粒的尺寸和形状因子，并且具有较好的耐磨性。振动斜板铸造材料比复合铸造材料具有更好的力学性能，这是因为基体中的碳化硅颗粒分布更加均匀，而且振动斜板铸造过程中形成了球形组织。

关键词：碳化硅增强 A356 铝基复合材料；复合铸造；振动斜板铸造；显微组织；颗粒分布；孔隙；硬度；耐磨性

(Edited by Xiang-qun LI)